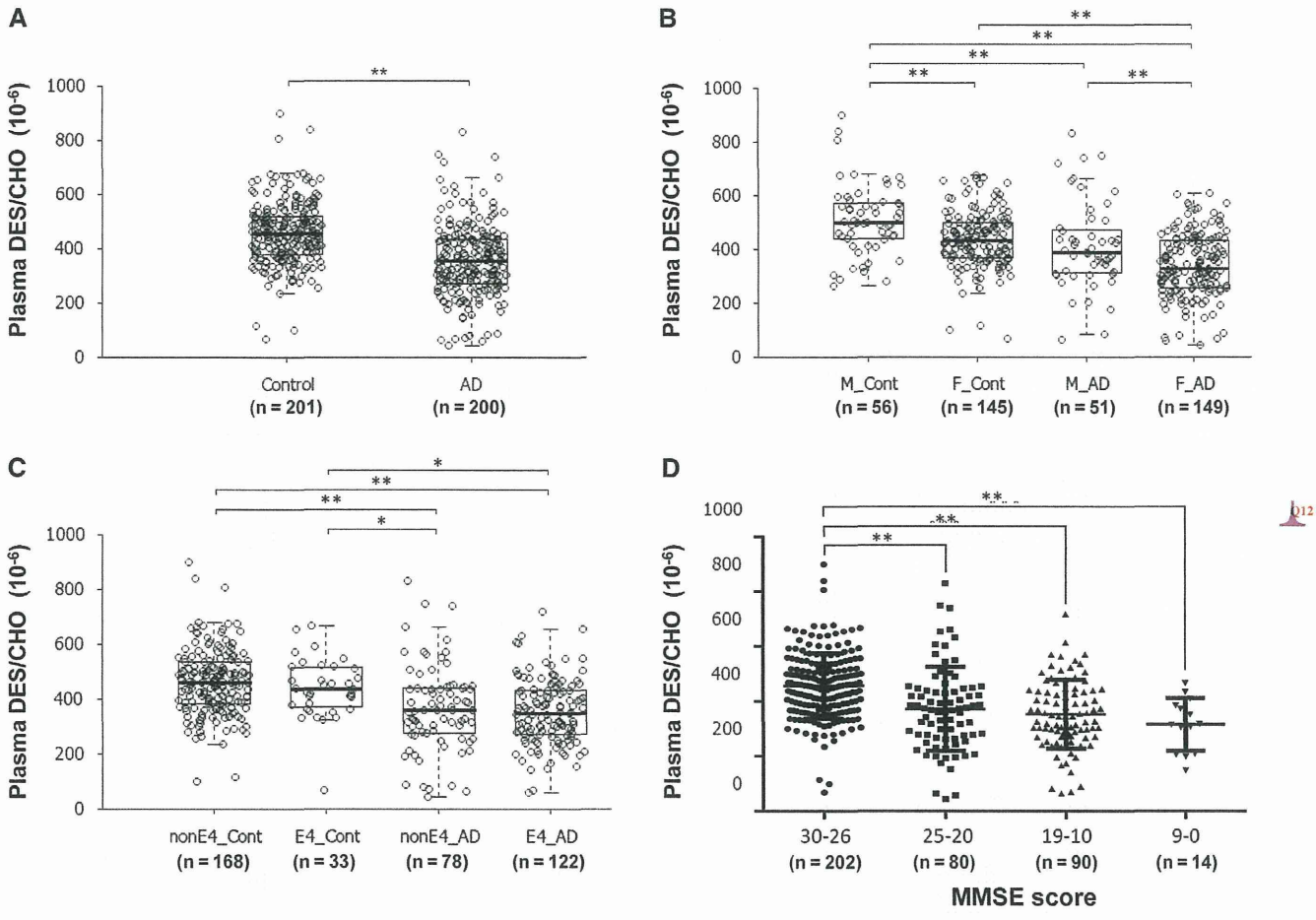

Fig. 1. Decreased plasma DES/CHO in patients with AD. (A) Comparison of plasma desmosterol-to-cholesterol ratio (DES/CHO) between 201 control and 200 AD subjects from a large Japanese cohort. (B) Comparison of plasma DES/CHO among male control (M_Cont), female control (F_Cont), male AD (M_AD), and female AD (F_AD) subjects. (C) Comparison of plasma DES/CHO between control subjects without *APOE* ε4 (nonE4_Cont) and with *APOE* ε4 (E4_Cont), and AD patients without *APOE* ε4 (nonE4_AD) and with *APOE* ε4 (E4_AD). (D) Comparison of plasma DES/CHO among groups classified as MMSE groups. $^{*}P < .05$; $^{**}P < .01$.

the mean change in MMSE score (change from the baseline) as threshold. Written informed consent was obtained from each of the participants (or the respective legal guardian); the study was approved by the appropriate university, hospital, and company institutional ethics committees.

2.2. Blood sampling and laboratory measurement

Peripheral blood samples were obtained from each participant using the commercially available blood collection tubes (Terumo Venoject for Japanese cohort) containing EDTA as the anticoagulant. Plasma was separated by centrifugation at 1500 *g* for 15 minutes at room temperature before being aliquoted and stored at −80°C until analysis.

The concentrations of desmosterol and cholesterol were measured with a liquid chromatography mass spectrometer (LC/MS), as described previously [7]. Briefly, 25 μL of plasma was spiked with cholesterol-25,26,26,26,27,27,27-D7 and desmosterol-26,26,26,27,27,27-D6 as internal standards. Fifty percent potassium hydroxide was then added to the solution, which was then mixed thoroughly and incubated at 70°C for 60 minutes. After the incubation, 2 mL of hexane and 0.5 mL of phosphate-buffered saline (pH 6.8) were added and mixed well. The solution was centrifuged for 10 minutes at 2000 *g*, and the upper organic phase was transferred to a new tube. The lower layer was extracted with an additional 1 mL of hexane, which was also added to the organic-phase extract. The solvents were evaporated to dryness under a nitrogen gas stream at 40°C, and the obtained pellet was reconstituted in ethanol and the resulting solution was subjected to LC/APCI-MS analysis as described previously [7].

2.3. Statistical analysis

Values are shown as mean ± standard deviation. Correlations between different variables were assessed using the Pearson correlation coefficient on log-transformed data. The *t* test or analysis of variance was carried out to determine differences between two or more groups. Nonparametric tests (Mann-Whitney *U* test) were carried out when the variables were not normally distributed. The paired *t* test was carried out to see the difference in the individual values

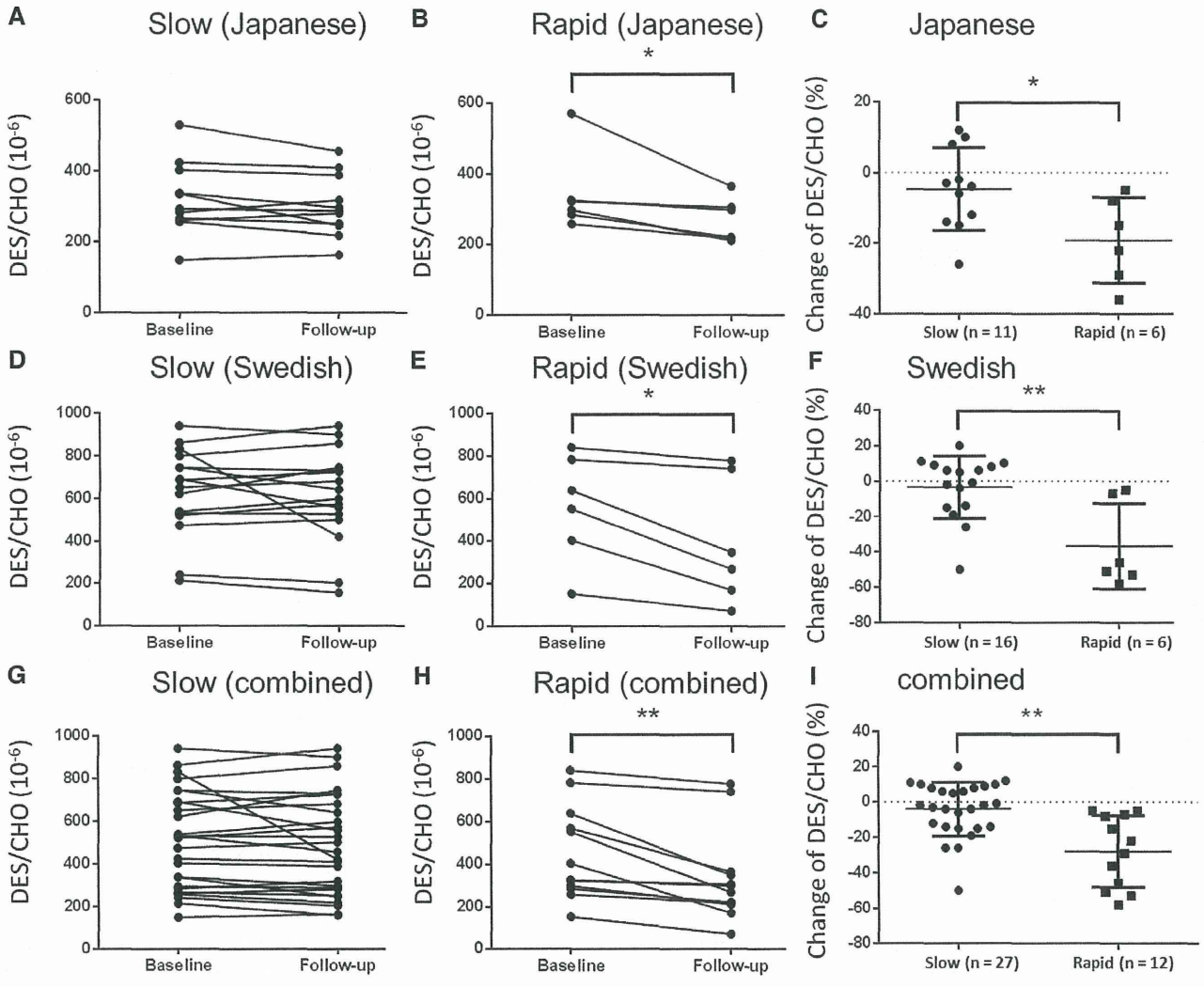

Fig. 2. Change in plasma DES/CHO between baseline and follow-up visits. AD/MCI subjects were classified into two groups, namely, those with slow progression (A, D, G) and those with rapid progression (B, E, H) on the basis of the mean ΔMMSE between baseline and follow-up visits in a Japanese cohort (A–C), a Swedish cohort (D–F), and a combined cohort (G–I). Plasma DES/CHO remains stable in the group with slow progression (A, D, G), whereas in the group with rapid progression, a significant decline over time was found (B, E, H). The change in plasma DES/CHO was significantly larger in the group with rapid progression than in the group with slow progression (C, F, I). *$P < .05$; **$P < .01$.

between baseline and follow-up visits. The statistical significance was set at $P < .05$.

3. Results

3.1. Cross-sectional study of plasma desmosterol

The characteristics of the AD and age-matched control subjects included in this cross-sectional study are listed in Table 1. A significant decline in plasma DES/CHO was observed in patients with AD compared with control subjects ($P < .01$; Fig. 1A). The decline in plasma DES/CHO in AD patients was significant regardless of gender or *APOE* ε4 status (Fig. 1B and C). There was a significant decline in plasma DES/CHO in AD patients with both the *APOE* ε3/3 and ε3/4 genotypes (data not shown; see Supplementary Fig. 1A and B for review). Plasma DES/CHO of female subjects in both the AD and control groups was significantly lower than that of male subjects (Fig. 1B, $P < .01$). No significant correlation of plasma DES/CHO with age was observed (data not shown). A significant correlation between plasma DES/CHO and MMSE score in both males and females was observed (data not shown; see Supplementary Fig. 1C and D for review). We divided subjects of this cohort into four MMSE score groups: high MMSE score (30 ≧ MMSE ≧ 26), middle MMSE score (25 ≧ MMSE ≧ 20), low MMSE score (19 ≧ MMSE ≧ 10), and very low MMSE score (9 ≧ MMSE ≧ 0). We then compared DES/CHO among these groups. A significant difference between the high MMSE score group and the other MMSE score groups was observed (Figure 1D).

The linear trend analysis revealed that there was also a significant change showing that groups with lower MMSE scores had lower DES/CHO (trend t test: $P < .01$).

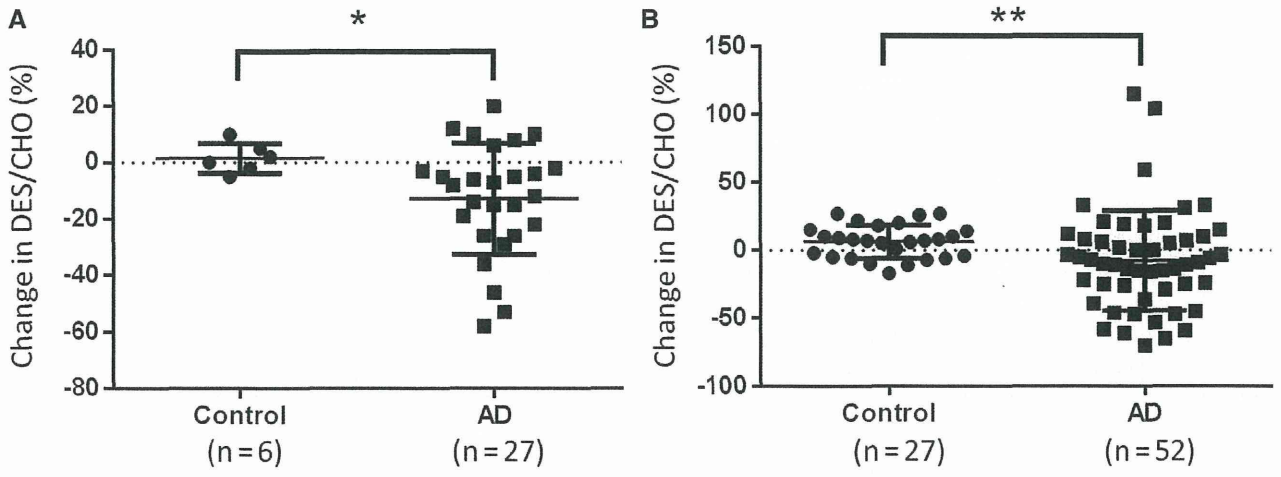

Fig. 3. Comparison of longitudinal change in plasma DES/CHO between control and AD subjects. (A) Longitudinal changes in plasma DES/CHO at two different points were compared between control subjects and AD patients from the combined cohort. *$P < .05$. (B) Longitudinal changes in plasma DES/CHO at multiple points were compared between control subjects and AD patients from the Swedish cohort and a commercially available resource. **$P < .01$.

3.2. Longitudinal analysis

Longitudinal plasma samples were collected from two clinical institutes, namely, Niigata University Hospital (Japanese cohort) and Uppsala University Hospital Memory Clinic (Swedish cohort). Forty-seven participants composed of 17 subjects in the Japanese cohort and 30 subjects in the Swedish cohort were included, and the demographic characteristics of these subjects are listed in Table 2. At baseline, DES/CHO in Japanese AD patients was significantly lower than that of Swedish AD patients ($P < .01$).

In the Japanese longitudinal cohort, the average change in the MMSE score (ΔMMSE) between the baseline and follow-up visits was -4 ± 4 with a change in DES/CHO of $-10 \pm 14\%$ (Table 2). Both MMSE score and plasma DES/CHO significantly decreased between the two visits in the Japanese cohort (paired t test, $P < .05$). In the Swedish cohort, the MMSE score (-3 ± 3) decreased significantly in AD patients between the baseline and follow-up visits ($P < .05$). However, in this cohort, there was no significant change in DES/CHO in both the AD patients and MCI subjects (Table 2). In the combined AD/MCI cohort, MMSE score (-2 ± 4) and plasma DES/CHO ($-11 \pm 20\%$) decreased significantly between the two visits (Table 2).

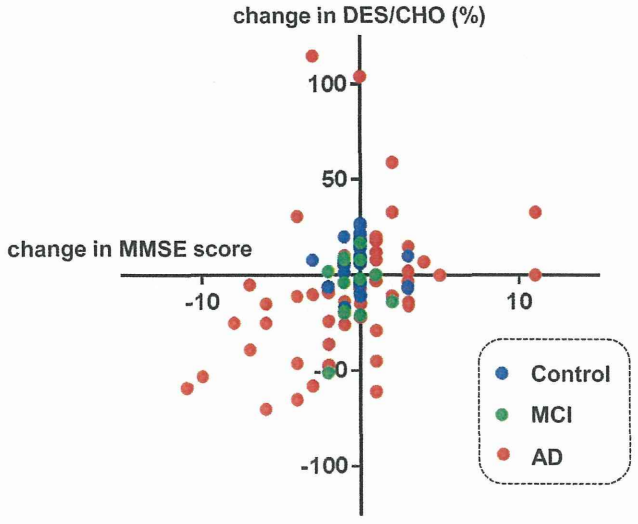

Fig. 4. Correlation between longitudinal changes in MMSE and plasma DES/CHO (%) in AD patients, MCI patients, and normal subjects. There were 122 points for blood collection, consisting of 30 baselines and 92 follow-ups (AD, 52 follow-ups; MCI, 13 follow-ups; and control, 27 follow-ups). There was a significant correlation between changes in MMSE and plasma DES/CHO (r = 0.37, $P < .01$).

Next, we divided the AD/MCI subjects into two groups, namely, those with slow or rapid progression, on the basis of their mean ΔMMSE in the Japanese (cutoff score, −4) and Swedish cohorts (cutoff score, −2) and compared the longitudinal change in plasma DES/CHO between groups (Fig. 2). Although the AD/MCI group with slow progression did not show any significant change in plasma DES/CHO (Fig. 2A, D, and G), groups with rapid progression showed a significant decrease in plasma DES/CHO between the baseline and follow-up visits (Fig. 2B, E, and H). In addition, the change in plasma DES/CHO was significantly larger in the AD/MCI group with rapid progression than in the group with slow progression in the Japanese, Swedish, and combined cohorts (Fig. 2C, F, and I).

We further compared the longitudinal change in plasma DES/CHO in control subjects and AD patients (Fig. 3). The change in DES/CHO between the two visits was -12.8 ± 19.7 in the AD patients, which was significantly larger than that in the control subjects (1.7 ± 5.3; Fig. 3A). These results suggest that although plasma DES/CHO in normal subjects remained stable, plasma DES/CHO in AD patients tended to decline over time.

Finally, we performed another longitudinal study to determine the association between plasma DES/CHO and ΔMMSE in 30 participants, including 18 AD, 6 MCI, and 6 control subjects from either the Swedish cohort or from PrecisionMed. Blood samples were collected every year or

every 6 months from the participants. There were 122 points for blood collection, consisting of 30 baselines and 92 follow-ups. The correlation between the ΔMMSE and the change in plasma DES/CHO (compared with baseline) determined using all 92 follow-up points is shown in Fig. 4. There was a significant correlation between the longitudinal ΔMMSE and the change in DES/CHO from the baseline ($P = .01, r = 0.37$). All the changes in MMSE score and plasma DES/CHO in each of the participants are shown (see Supplementary Fig.2 for review). In addition, AD patients showed a significant decrease in plasma DES/CHO at follow-up intervals ($-7.7 \pm 36.8\%$) compared with the control subjects ($6.4 \pm 12.3\%$) in this cohort (Fig. 3B).

4. Discussion

The present cross-sectional study using a Japanese cohort was undertaken to replicate our previous finding that plasma DES/CHO is decreased in Caucasian patients with AD. The following points were confirmed in the present Japanese and previously reported Caucasian cross-sectional cohorts: (1) plasma DES/CHO was decreased in patients with AD in comparison with control subjects, (2) the decrease in plasma DES/CHO in AD patients was independent of gender and *APOE* genotype, (3) female subjects tended to have a lower plasma DES/CHO than male subjects, and (4) plasma DES/CHO correlated significantly with the MMSE score. Taken together, the results suggest that plasma DES/CHO may be a potential diagnostic biomarker reflecting cognitive dysfunction in AD patients.

Recently, Popp et al. [17] have reported that the plasma desmosterol level does not change in AD patients. The discrepancy in finding between that and the present study may be explained by differences in the analytical methods used to determine the concentration of desmosterol. We previously showed that the LC/MS method that we used in the present study enables the purification of desmosterol in plasma more efficiently than the gas chromatography method used in the study by Popp et al. [7,17]. Thus, the LC/MS method is likely to be more suitable for the measurement of plasma desmosterol concentration.

Here, we determined for the first time the longitudinal change in plasma DES/CHO and examined a possible association with concurrent cognitive decline in AD/MCI patients. Our results revealed (1) that plasma DES/CHO was relatively stable over time in cognitively normal controls, whereas it significantly decreased in AD patients; (2) a more pronounced decline in plasma DES/CHO in the AD/MCI group with rapid progression than in the group with slow progression; and (3) that the longitudinal change in plasma DES/CHO positively correlated with the change in the MMSE score. These results suggest that the plasma DES/CHO change is associated with the cognitive decline in AD and might be used to monitor the progression of cognitive decline in patients with AD. It will be interesting to clarify the usefulness of monitoring plasma DES/CHO as a surrogate marker for evaluating the effects of clinical drug trials in patients with AD.

Our longitudinal study suggests that the plasma DES/CHO changes before the appearance of clinical symptoms, as determined by MMSE in some cases (see Supplementary Fig. 2 for review; subjects A, C, and H). The result obtained from the subject with MCI that converted to AD (see Supplementary Fig. 2 for review; subject S) may suggest that plasma DES/CHO is useful as a progression marker to monitor the conversion from MCI to AD. In this connection, recent lipidomic analysis showed that the quantification of several lipid metabolites in plasma, such as phosphatidylcholine and acylcarnitine, is useful for predicting phenoconversion to amnestic MCI or AD in cognitively normal subjects [18].

There is now accumulating evidence that cholesterol metabolism may be relevant to the production and clearance of Aβ and thus to the Aβ-related toxicity in the pathogenesis of AD [19]. The strongest genetic risk factor for sporadic AD is the ε4 allele of *APOE*, which encodes apolipoprotein E (apoE), with a crucial role in cholesterol metabolism [20]. The presence of *APOE* ε4 may contribute to the pathologic accumulation and deposition of cerebral Aβ at early preclinical disease stages [21]. A recent study has shown that CSF apoE levels are decreased in patients with AD and that MCI in subjects with a low CSF apoE level will more likely convert to AD [22]. An interaction between *APOE* genotype and plasma desmosterol level may be postulated because desmosterol is the immediate precursor of cholesterol. However, the plasma desmosterol level was not clearly associated with *APOE* genotype in this study.

It is of particular interest that the level of desmosterol in the AD brain was found to be lower than that of control brain [7,23]. It has been demonstrated that the levels of steroid hormones (e.g., progesterone, pregnenolone, and 17αOH-progesterone) that exhibit inhibitory activity against DHCR24 are decreased in the AD brain, particularly in the vicinity of plaques and neurofibrillary tangles [24]. Notably, the concentration of desmosterol is 100-fold higher in the rat brain than in the rat liver [25], which implies that most of the desmosterol in the blood might originate from the brain. Taken together, it could be speculated that brain desmosterol level may decrease with an increase in DHCR24 activity in the AD brain; this may subsequently result in a change in plasma DES/CHO. The question of why plasma DES/CHO decreases in patients with AD and is associated with longitudinal cognitive decline in the course of the disease warrants further investigation.

Although our findings, using samples from cross-sectional and longitudinal cohorts, are interesting, our study has some limitations. We did not analyze the samples from other types of dementia, including dementia with Lewy bodies, frontotemporal dementia, and vascular dementia. An additional cross-sectional study that includes samples from other types of dementia will be necessary. The number of samples from longitudinal cohorts in this study is relatively small. Longitudinal studies with a prospective design using a larger number

of samples should be performed to confirm the utility of plasma DES/CHO as a longitudinal biomarker. Moreover, it is important to understand how early plasma DES/CHO starts to decline using longitudinal samples from asymptomatic AD subjects with amyloid deposition confirmed by amyloid-PET imaging. Although our findings need to be validated in independent cohorts, our data suggest that the use of plasma desmosterol as a blood biomarker can be useful in the diagnosis of AD and also in monitoring disease progression.

Acknowledgments

The authors would like to thank the subjects who participated in this study. We would like to thank Dr. Makoto Ogo and Mr. Mamoru Yanagimachi who provided valuable comments. Special thanks also go to Mr. Kentaro Matsuura and Mr. Masayuki Ikawa whose support and information have helped us throughout this study. This study was funded by grants from Eisai Co. Ltd., Japanese Society of Promotion of Science, Ministry of Health, Labour and Welfare, Japan, and Uppsala University.

Supplementary data

Supplementary data related to this article can be found at http://dx.doi.org/10.1016/j.dadm.2014.11.009.

RESEARCH IN CONTEXT

1. Systemic review: There is a compelling need to establish blood-based biomarker to diagnose Alzheimer's disease (AD) and monitor the disease progression. A previous study reported that plasma desmosterol-to-cholesterol ratio (DES/CHO) is significantly decreased in Caucasian patients with AD.
2. Interpretation: We found that plasma DES/CHO was significantly reduced in Japanese AD patients. The longitudinal study revealed (1) that plasma DES/CHO was relatively stable in normal controls, whereas it significantly decreased in AD patients; (2) a more pronounced decline in plasma DES/CHO in the AD/MCI group with rapid progression than in that with slow progression; and (3) that the longitudinal change in plasma DES/CHO positively correlated with the change in MMSE score.
3. Future directions: A future cross-sectional study that includes samples from other types of dementia and longitudinal studies with a prospective design using a larger number of samples need to be performed to confirm the utility of plasma DES/CHO.

References

[1] Sperling RA, Aisen PS, Beckett LA, Bennett DA, Craft S, Fagan AM, et al. Toward defining the preclinical stages of Alzheimer's disease: recommendations from the National Institute on Aging-Alzheimer's Association workgroups on diagnostic guidelines for Alzheimer's disease. Alzheimers Dement 2011;7:280–92.
[2] Blennow K, Hampel H. CSF markers for incipient Alzheimer's disease. Lancet Neurol 2003;2:605–13.
[3] Jack CR Jr, Holtzman DM. Biomarker modeling of Alzheimer's disease. Neuron 2013;80:1347–58.
[4] Sutphen CL, Fagan AM, Holtzman DM. Progress update: Fluid and imaging biomarkers in Alzheimer's disease. Biol Psychiatry 2014;75:520–6.
[5] Rosen C, Hansson O, Blennow K, Zetterberg H. Fluid biomarkers in Alzheimer's disease—current concepts. Mol Neurodegener 2013;8:20.
[6] Blennow K, Hampel H, Weiner M, Zetterberg H. Cerebrospinal fluid and plasma biomarkers in Alzheimer disease. Nat Rev Neurol 2010;6:131–44.
[7] Sato Y, Suzuki I, Nakamura T, Bernier F, Aoshima K, Oda Y. Identification of a new plasma biomarker of Alzheimer's disease using metabolomics technology. J Lipid Res 2012;53:567–76.
[8] Hinse CH, Shah SN. The desmosterol reductase activity of rat brain during development. J Neurochem 1971;18:1989–98.
[9] Couillard-Despres S, Iglseder B, Aigner L. Neurogenesis, cellular plasticity and cognition: the impact of stem cells in the adult and aging brain—a mini-review. Gerontology 2011;57:559–64.
[10] Jinno S. Decline in adult neurogenesis during aging follows a topographic pattern in the mouse hippocampus. J Comp Neurol;519:451–466.
[11] McKhann G, Drachman D, Folstein M, Katzman R, Price D, Stadlan EM. Clinical diagnosis of Alzheimer's disease: report of the NINCDS-ADRDA Work Group under the auspices of Department of Health and Human Services Task Force on Alzheimer's Disease. Neurology 1984;34:939–44.
[12] Folstein MF, Folstein SE, McHugh PR. "Mini-mental state". A practical method for grading the cognitive state of patients for the clinician. J Psychiatr Res 1975;12:189–98.
[13] Kuwano R, Miyashita A, Arai H, Asada T, Imagawa M, Shoji M, et al. Dynamin-binding protein gene on chromosome 10q is associated with late-onset Alzheimer's disease. Hum Mol Genet 2006;15:2170–82.
[14] Petersen RC, Morris JC. Mild cognitive impairment as a clinical entity and treatment target. Arch Neurol 2005;62:1160–3. discussion 7.
[15] Petersen RC, Smith GE, Waring SC, Ivnik RJ, Tangalos EG, Kokmen E. Mild cognitive impairment: clinical characterization and outcome. Arch Neurol 1999;56:303–8.
[16] Giedraitis V, Sundelof J, Irizarry MC, Garevik N, Hyman BT, Wahlund LO, et al. The normal equilibrium between CSF and plasma amyloid beta levels is disrupted in Alzheimer's disease. Neurosci Lett 2007;427:127–31.
[17] Popp J, Meichsner S, Kolsch H, Lewczuk P, Maier W, Kornhuber J, et al. Cerebral and extracerebral cholesterol metabolism and CSF markers of Alzheimer's disease. Biochem Pharmacol 2013;86:37–42.
[18] Mapstone M, Cheema AK, Fiandaca MS, Zhong X, Mhyre TR, Macarthur LH, et al. Plasma phospholipids identify antecedent memory impairment in older adults. Nat Med 2014;20:415–8.
[19] Di Paolo G, Kim TW. Linking lipids to Alzheimer's disease: cholesterol and beyond. Nat Rev Neurosci 2011;12:284–96.
[20] Bu G. Apolipoprotein E and its receptors in Alzheimer's disease: pathways, pathogenesis and therapy. Nat Rev Neurosci 2009;10:333–44.
[21] Kok E, Haikonen S, Luoto T, Huhtala H, Goebeler S, Haapasalo H, et al. Apolipoprotein E-dependent accumulation of Alzheimer

disease-related lesions begins in middle age. Ann Neurol 2009; 65:650–7.
[22] Toledo JB, Da X, Weiner MW, Wolk DA, Xie SX, Arnold SE, et al. CSF Apo-E levels associate with cognitive decline and MRI changes. Acta Neuropathol 2014;127:621–32.
[23] Wisniewski T, Newman K, Javitt NB. Alzheimer's disease: brain desmosterol levels. J Alzheimers Dis 2013;33:881–8.
[24] Lindenthal B, Holleran AL, Aldaghlas TA, Ruan B, Schroepfer GJ Jr, Wilson WK, et al. Progestins block cholesterol synthesis to produce meiosis-activating sterols. FASEB J 2001;15:775–84.
[25] Smiljanic K, Vanmierlo T, Djordjevic AM, Perovic M, Loncarevic-Vasiljkovic N, Tesic V, et al. Aging induces tissue-specific changes in cholesterol metabolism in rat brain and liver. Lipids 2013; 48:1069–77.

INTERNAL MEDICINE

□ CASE REPORT □

A Second Pedigree with Amyloid-less Familial Alzheimer's Disease Harboring an Identical Mutation in the *Amyloid Precursor Protein* Gene (E693delta)

Yumiko Kutoku[1], Yutaka Ohsawa[1], Ryozo Kuwano[2], Takeshi Ikeuchi[2], Haruhisa Inoue[3], Suzuka Ataka[4], Hiroyuki Shimada[4], Hiroshi Mori[5] and Yoshihide Sunada[1]

Abstract

A 59-year-old woman developed early-onset, slowly progressive dementia and spastic paraplegia. positron emission tomography (PET) imaging revealed a large reduction in the level of glucose uptake without amyloid deposition in the cerebral cortex. We identified a homozygous microdeletion within the amyloid β (Aβ) coding sequence in the *amyloid precursor protein* (*APP*) gene (c.2080_2082delGAA, p.E693del) in three affected siblings and a heterozygous microdeletion in an unaffected sibling. The identical mutation was previously reported in the first Alzheimer's pedigree without amyloid deposits. Furthermore, an increase in high-molecular-weight Aβ-reactive bands was detected in the patient's CSF. Our findings suggest that soluble Aβ-oligomers induce neuronal toxicity, independent of insoluble Aβ fibrils.

Key words: Alzheimer's disease, familial Alzheimer's disease, *APP* gene, Aβ oligomers, PET

(Intern Med 54: 205-208, 2015)
(DOI: 10.2169/internalmedicine.54.3021)

Introduction

Alzheimer's disease (AD) is distinguished pathologically from other forms of dementia by amyloid deposition in the brain (1). Amyloid deposits are comprised of insoluble fibrils of 40 and 42-residue amyloid β (Aβ) peptides, derived from the amyloid precursor protein (APP). To date, approximately 40 missense mutations in the *APP* gene have been identified in over 80 AD families, most of which are located near processing sites or within the Aβ coding sequence (2). Almost all mutations in the *APP* gene cause the disease in a dominant manner, suggesting that these mutations confer a gain-of-function that results in the enhanced formation and deposition of insoluble Aβ fibrils (3, 4). However, one AD pedigree was reported to have a single amino acid deletion within the Aβ coding sequence (E693delta), inherited as a recessive trait, with a lack of Aβ deposition (5). Recently, soluble Aβ oligomers, the precursors of insoluble Aβ fibrils, have been suggested to play a pivotal role in the pathogenesis of AD (6, 7). In this study, we report a second recessive AD pedigree negative for amyloid plaque, harboring the identical E693 deletion. Our findings suggest a link between this recessive mutation and the enhanced formation of soluble Aβ oligomers.

Case Report

We examined three patients from a single generation in a pedigree from an isolated island in the Seto Inland Sea, Japan (Fig. 1A). The subjects' parents were first cousins and had no history of apparent episodes of memory or motor impairment.

The proband (II-8) was a 59-year-old woman admitted to our hospital for treatment of aspiration pneumonia. She had been well until 35 years of age, when her family members

[1]Department of Neurology, Kawasaki Medical School, Japan, [2]Department of Molecular Genetics, Bioresource Science Branch, Center for Bioresources, Brain Research Institute, Niigata University, Japan, [3]Center for iPS Cell Research and Application, Kyoto University, Japan, [4]Department of Geriatrics and Neurology, Osaka City University Graduate School of Medicine, Japan and [5]Department of Neuroscience, Osaka City University Graduate School of Medicine, Japan
Received for publication April 7, 2014; Accepted for publication May 29, 2014
Correspondence to Dr. Yoshihide Sunada, ysunada@med.kawasaki-m.ac.jp

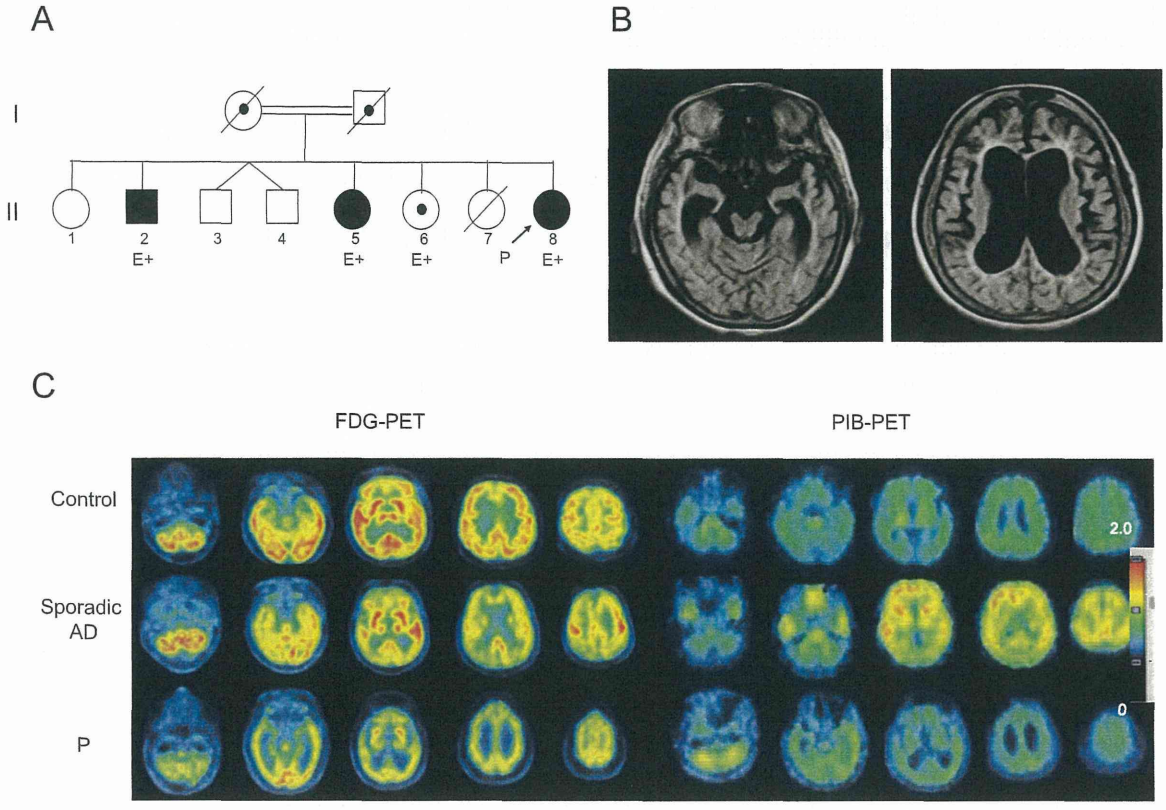

Figure 1. An AD patient negative for amyloid deposition. (A) Pedigree chart. The proband is indicated by a "P." A closed square or circle represents an affected member. A square or circle with a dot in the middle represents an obligate carrier. A genetic study of the *APP* gene was performed in members marked with "E+." (B) MRI FLAIR images of the brain of the proband at 50 years of age. (C) PET images showing glucose uptake [(^{18}F)-fluorodeoxyglucose, FDG; left] and amyloid deposition [(^{11}C)-Pittsburgh compound-B, PIB; right] in the brain. Control: a 78-year-old man without dementia (upper). Sporadic AD: a 78-year-old woman with sporadic Alzheimer's disease (middle). P: the proband at 59 years of age (lower).

noticed short-term memory disturbances, particularly as she took her dog for a walk numerous times each day. She was diagnosed with AD at 42 years of age based on progressive cognitive impairment and prominent spatial disorientation. At 48 years of age, she first complained of difficulty walking in a straight line and consequently required a wheelchair for mobility. She became bedridden with urinary incontinence by 50 years of age. She was mute and unable to obey simple commands. She was admitted to our hospital at 56 years of age, at which time she had spastic paraparesis and mild dysphagia. The Aβ level in the serum and the total and phosphorylated tau levels in the cerebrospinal fluid (CSF) were normal. Fluid-attenuated inversion-recovery (FLAIR) magnetic resonance imaging (MRI) imaging showed remarkable brain shrinkage at 56 years of age (Fig. 1B). [^{18}F]-fluorodeoxyglucose (FDG) positron emission tomography (PET) revealed a greater reduction in the level of glucose uptake in the cerebral cortex compared to that observed in sporadic AD patients, suggesting severely impaired energy metabolism in the cerebral cortex (Fig. 1C, left). Unexpectedly, PET amyloid images using [^{11}C]-Pittsburg compound-B (PIB) (8) were negative for amyloid deposition, comparable to that noted in normal control subjects (Fig. 1C, right).

Patients II-2 and II-5, the 76-year-old brother and 65-year-old sister of the proband, respectively, had milder clinical signs and symptoms than the proband. The onset of memory impairment in the brother and sister at 59 and 44 years of age, respectively, was succeeded by difficulty in walking due to spasticity of the lower limbs at 66 and 58 years of age, respectively. Both patients exhibited spastic paraparesis and mutism and were being treated at other hospitals.

The local ethics committee approved the present genetic study (No. 552-1), which was performed with informed consent from an unaffected sibling (II-6) and the spouses of the affected siblings (II-8, II-2, II-5). By sequencing exons 16 and 17 of the *APP* gene, we identified a homozygous microdeletion (c.2080_2082delGAA, p.E693del) in the affected siblings, whereas the unaffected sibling had a heterozygous deletion. Codon 693 in the *APP* gene codes for amino acid protein 22 (E22) of the Aβ peptide (Fig. 2A). The proband displayed normal sequences for all exons in two presenilin genes (*PSEN1* and *PSEN2*), with an *APOE* genotype of ε3/ε3.

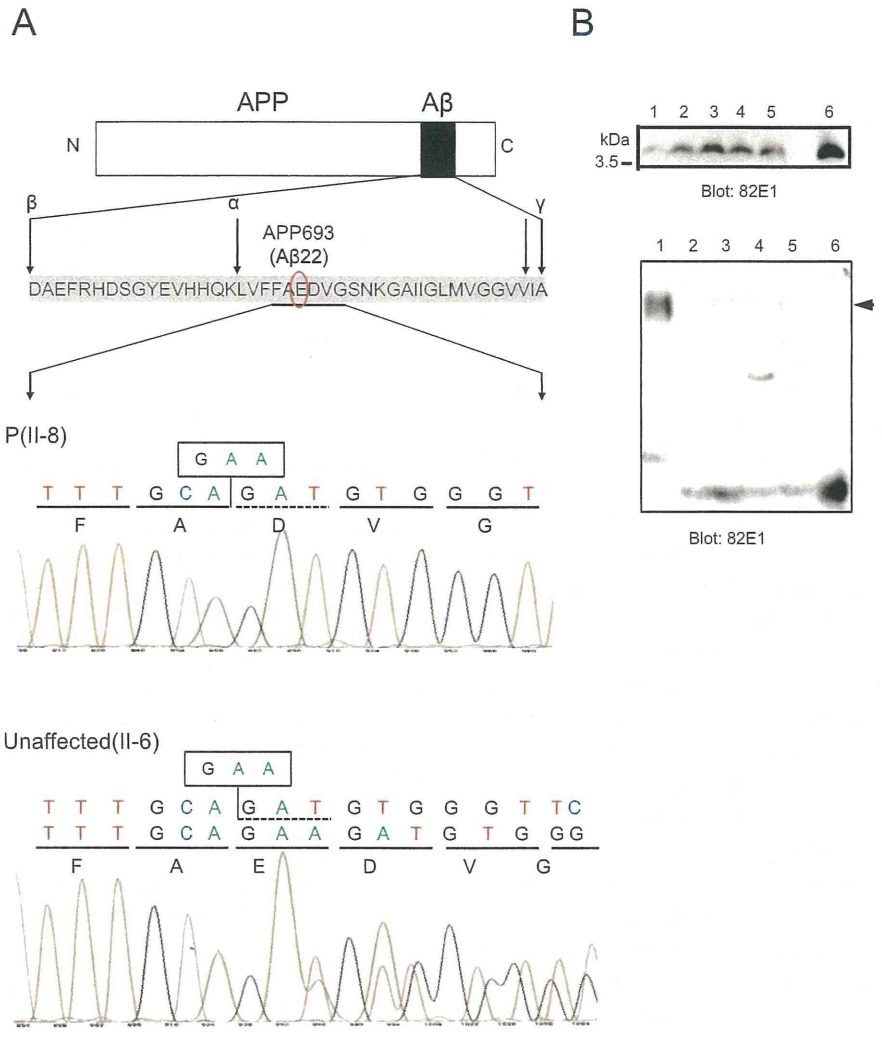

Figure 2. DNA and protein analyses. (A) Schematic representation of the APP protein structure (upper). The amino acid E693 in the APP protein corresponds to amino acid E22 of the Aβ peptide (Aβ22, middle). DNA sequences of the proband (P, II-8; lower) and an unaffected sibling (Unaffected, II-6; lower) are shown. The microdeletion of the *APP* gene and the deduced amino acid sequence of the APP protein are shown. (B) Increased formation of high-molecular-weight bands reactive against the anti-Aβ antibody in the CSF obtained from the proband. Aliquots of CSF obtained from the proband (lane 1) or normal control subjects (lanes 2-5) were size fractionated under denaturing (upper) or non-denaturing (lower) conditions and subsequently immunoblotted with a mouse monoclonal anti-Aβ antibody (82E1). This analysis showed the enhanced formation of high-molecular-weight Aβ products (visible as diffuse banding) under non-denaturing conditions in the CSF obtained from the proband (arrowhead, lower), despite a reduction in the level of total Aβ under denaturing conditions (upper). Synthetic Aβ peptides were run on the same gel for comparison purposes (lane 6).

We then examined the level of Aβ in the CSF sample obtained from the proband. An immunoblot analysis using an anti-Aβ antibody was performed under both denaturing and non-denaturing conditions. Compared to the control levels, the total Aβ level was decreased under the denaturing conditions (Fig. 2B, upper panel). Interestingly, however, non-denaturing electrophoresis demonstrated the levels of high-molecular-weight bands recognized by the anti-Aβ antibody to be markedly elevated in the proband (Fig. 2B, lower panel), thus suggesting enhanced formation of soluble Aβ oligomers.

Discussion

In this report, we described a recessive familial AD pedigree harboring a single amino acid deletion mutation (E693 delta) within the *APP* gene, identical to one previously reported (5). The most remarkable phenotypic features of this mutation are the lack of amyloid deposition and increased soluble Aβ oligomers in the CSF. It may be inappropriate to categorize this form of dementia without amyloid deposition as AD; however, recent findings indicate that Aβ oligomers

play a critical role in synaptic dysfunction, at least in the early stage of AD (9-11). This case report further indicates that Aβ oligomers induce neuronal degeneration without amyloid deposition. Because abnormal metabolism of *APP* or Aβ is a molecular pathogenetic feature in the current pedigree, our subjects can be diagnosed to be within the range of the AD spectrum.

It remains unclear whether Aβ oligomers accumulate in synapses or somata or how they impair synaptic transmission and induce neuronal dysfunction (12). A synthetic E693 delta Aβ peptide was recently shown to facilitate Aβ oligomerization, although this did not lead to Aβ fibrillization (5). Additionally, *APP*-E693delta transgenic mice exhibit a brain pathology partially resembling that of AD, including the presence of intracellular Aβ oligomers, although without extracellular Aβ deposition (12). Indeed, the CSF obtained from the current proband showed an increased level of high-molecular-weight Aβ-reactive bands, presumably corresponding to toxic $A\beta_{40/42}$ oligomers. In accordance with that observed in the first report of this condition, the homozygous E693 deletion of the *APP* gene in this pedigree may cause dementia solely via the formation of toxic Aβ oligomers, not the deposition of insoluble Aβ fibrils.

Kinship with the previously reported pedigree (5) is not clear in our investigation, which was limited to the identification of second- and third-degree relatives of the proband. Compared with the patient in the first report (5), our proband exhibited an earlier onset of dementia (33 vs. 55 years), more profound motor impairment (paraplegia vs. mild pyramidal tract signs) and more severe brain shrinkage (whole brain atrophy vs. parietal lobe atrophy). Other differences in genetic background may modify the severity of these phenotypes. Further studies are therefore required to clarify the pathogenetic mechanisms underlying the phenotypic differences caused by identical amino acid deletions.

The authors state that they have no Conflict of Interest (COI).

Financial Support

Dr. Ohsawa received support from the Japan Society for the Promotion of Science (C-20591013, C-23591261, C-26461285), National Center of Neurology and Psychiatry (23-5, 26-8) and Kawasaki Medical School (22-A24, 23-B60). Dr. Sunada received support from the Japan Society for the Promotion of Science (C-21591101), National Center of Neurology and Psychiatry (20B-13), Ministry of Health, Labour and Welfare of Japan (H20-018) and Kawasaki Medical School (22-T1, 23-P1).

References

1. Bettens K, Sleegers K, Van Broeckhoven C. Current status on Alzheimer disease molecular genetics: from past, to present, to future. Hum Mol Genet **15** (19 R1): R4-R11, 2010.
2. Alzforum Networking for a Cure. Mutations [Internet]. [cited 2014 Apr 3]. Available from: http://www.alzforum.org
3. Citron M, Oltersdorf T, Haass C, et al. Mutation of the beta-amyloid precursor protein in familial Alzheimer's disease increases beta-protein production. Nature **360**: 672-674, 1992.
4. Di Fede G, Catania M, Morbin M, et al. A recessive mutation in the *APP* gene with dominant-negative effect on amyloidogenesis. Science **323**: 1473-1477, 2009.
5. Tomiyama T, Nagata T, Shimada H, et al. A new amyloid beta variant favoring oligomerization in Alzheimer's-type dementia. Ann Neurol **63**: 377-387, 2008.
6. Selkoe DJ. Alzheimer's disease is a synaptic failure. Science **298**: 789-791, 2002.
7. Mattson MP. Pathways towards and away from Alzheimer's disease. Nature **430**: 631-639, 2004.
8. Klunk WE, Engler H, Nordberg A, et al. Imaging brain amyloid in Alzheimer's disease with Pittsburgh Compound-B. Ann Neurol **55**: 306-319, 2004.
9. Walsh DM, Klyubin I, Fadeeva JV, et al. Naturally secreted oligomers of amyloid beta protein potently inhibit hippocampal long-term potentiation in vivo. Nature **416**: 535-539, 2002.
10. Larson ME, Lesné SE. Soluble Aβ oligomer production and toxicity. J Neurochem **120** Suppl 1: 125-139, 2012.
11. Benilova I, Karran E, De Strooper B. The toxic Aβ oligomer and Alzheimer's disease: an emperor in need of clothes. Nat Neurosci **15**: 349-357, 2012.
12. Kondo T, Asai M, Tsukita K, et al. Modulating Alzheimere's disease with iPSCs reveals stress phenotypes associated with intracellular Aβ and differential responsiveness. Cell Stem Cell **12**: 487-496, 2013.

Reduction of water influx into CSF in Alzheimer's disease, supporting the β-amyloid clearance hypothesis

Yuji Suzuki, MD, PhD[1], Yukihiro Nakamura, PhD[1], Kenichi Yamada, MD, PhD[1], Hironaka Igarashi, MD PhD[1], Kensaku Kasuga, MD, PhD[2], Yuichi Yokoyama, MD[4], Takeshi Ikeuchi, MD. PhD[2], Masatoyo Nishizawa, M.D., Ph.D.[3], Ingrid L. Kwee, MD[5], and Tsutomu Nakada, MD, PhD, FAAN, FANA[1,5]

Center for Integrated Human Brain Science[1] and Departments of Molecular Genetics[2] and Neurology[3], Brain Research Institute, University of Niigata

Department of Psychiatry, Faculty of Medicine, University of Niigata[4]

Department of Neurology, University of California, Davis[4]

Word Count for the Paper: 1392
Word Count for the Abstract: 237
Character Count for the Title: 90
Number of References: 22
Number of Tables: 1
Number of Figures: 1

Correspondence:
Tsutomu Nakada, M.D., Ph.D., FAAN, FANA
Center for Integrated Human Brain Science
Brain Research Institute, University of Niigata
1-757 Asahimachi, Niigata, 951-8585, Japan
E-mail: tnakada@bri.niigata-u.ac.jp, URL: coe.bri.niigata-u.ac.jp
Tel: +81-25-227-0677, Fax: +81-25-227-0822

Contribution:

Yuji Suzuki, MD, PhD: yuji-s@bri.niigata-u.ac.jp
Drafting/revision the manuscript
Acquisition of data
Statistical analysis

Yukihiro Nakamura, PhD: nakamura@bri.niigata-u.ac.jp
Analysis or interpretation of data
Acquisition of data

Kenichi Yamada, MD, PhD: yamadak@bri.niigata-u.ac.jp
Analysis or interpretation of data
Acquisition of data

Hironaka Igarashi, MD PhD: higara@bri.niigata-u.ac.jp
Analysis or interpretation of data
Statistical analysis

Kensaku Kasuga, MD, PhD: ken39@bri.niigata-u.ac.jp
Analysis or interpretation of data

Yuichi Yokoyama, MD: yokoyama@med.niigata-u.ac.jp
Analysis or interpretation of data

Takeshi Ikeuchi, MD. PhD: ikeuchi@bri.niigata-u.ac.jp
Analysis or interpretation of data

Masatoyo Nishizawa, MD. PhD: nishi@bri.niigata-u.ac.jp
Analysis or interpretation of data

Ingrid L. Kwee, MD: ilkwee@ucdavis.edu
Drafting/revision the manuscript
Analysis or interpretation of data

Tsutomu Nakada, MD, PhD, FAAN, FANA: tnakada@bri.niigata-u.ac.jp
Study concept or design
Drafting/revision the manuscript
Analysis or interpretation of data
Obtaining funding

Disclosure:

All authors have nothing to disclose.

Funding:

The study was supported by grants from the Ministry of Education, Culture, Sports, Science, and Technology (Japan) and University of Niigata.

Abstract

Objectives

To investigate whether water influx into cerebrospinal fluid (CSF) space is reduced in Alzheimer's patients as had been previously shown in transgenic Alzheimer's disease model mice.

Methods

Ten normal, young volunteers (young control, 21-24 years old), ten normal, senior volunteers (senior control, 60-78 years old, MMSE $\geqq$ 29), and ten Alzheimer's disease (AD) patients (study group, 59-84 years old, MMSE: 13-19) participated in this study. All AD patients were diagnosed by neurologists specialized in dementia based on DSM-IV criteria. CSF dynamics were analyzed using positron emission tomography (PET) following an intravenous injection of 1,000 MBq [15O]H2O synthesized on-line.

Results

Water influx into CSF space in AD patients expressed as influx ratio (0.755 ± 0.089) was significantly reduced compared to both young controls (1.357 ± 0.185, $p < 0.001$) and senior controls (0.901 ± 0.253, $p < 0.05$). Influx ratio in senior controls compared to that in young control was found to be significantly reduced ($p< 0.01$) as well. The large range of influx ratio observed in senior controls (0.599-1.442) suggests that reduction in water influx into CSF represents one of the aging processes.

Conclusion

Reduction in water influx into the CSF and, hence, clearance rate of β-amyloid appears to be the necessary, if not sufficient, factor in the pathogenesis of AD. Cohort studies for assessing dynamical indices of the balance between production and clearance of β-amyloid in various populations, including mild cognitive impairment (MCI), are warranted.

Introduction

The brain lacks a conventional lymphatic system responsible for clearing interstitial fluid (ISF) of solutes not absorbed across capillaries. The cerebrospinal flow (CSF) system has long been suggested to play a role equivalent to systemic lymphatics. Nevertheless, the classical CSF circulation theory is not totally compatible with the notion, and the role of CSF as the brain's lymphatic system has not received much attention. Recently, however, the circulation theory where CSF is almost exclusively produced by choroid plexus has come under serious challenge. It is now understood that CSF is produced and absorbed throughout the entire CSF system, and the peri-capillary (Virchow-Robin) space plays a critical role[1-3].

A number of studies have now shown that CSF flow through the Virchow Robin space (interstitial flow of the brain) plays a critical role in the clearance of β-amyloid[4-8]. Prealbumin (transthyretin) in the CSF is found to be a chaperon for β-amyloid, and prevents β-amyloid's natural tendency to form into plaques[9]. It is conceivable that disturbance of water influx into the CSF may play a significant, if not sole, role in the pathogenesis of senile plaque (SP) formation and, hence, Alzheimer's disease (AD).

Water homeostasis of the Virchow-Robin space and, therefore, interstitial flow is regulated by aquaporin-4 (AQP-4)[2,3,10], an isoform of water channels abundant in the brain. Using a newly developed non-invasive magnetic resonance imaging (MRI) method capable of tracing exogenously applied substrates similar to positron emission tomography (PET)), JJ vicinal coupling proton exchange (JJVCPE) imaging[11-12], we successfully demonstrated that water influx into the CSF system is indeed regulated by the AQP-4 system[2]. This influx is significantly reduced in senile plaque bearing transgenic AD model mice to the extent similar to AQP-4 knockout mice[13-14]. In this study, we confirmed this finding in AD patients using positron emission tomography (PET).

Materials and Methods

Subjects

Ten normal, young volunteers (age 21-24 years), ten normal, senior volunteers (age 60-78 years), and ten Alzheimer's disease (AD) patients (age 59-84 years) participated in this study. All AD patients, diagnosed by neurologists specialized in dementia based on DSM-IV criteria, were recruited from the Niigata University Hospital. Age-matched senior volunteers were assessed to have no functional and no cognitive impairment (Mini-Mental State Examination (MMSE) score $\geqq$29), and had no neurological disease. Written informed consent was obtained from all subjects or their proxy. Studies were

performed according to the human research guidelines of the Internal Review Board of University of Niigata. The project was registered at the UMIN Clinical Trials Registry as UMIN000011939 (http://www.umin.ac.jp/ctr/index.htm).

PET imaging

PET imaging was performed using a combined PET/CT scanner (Discovery ST Elite, GE Healthcare, Schenectady NY, USA) with a 15 cm field of view (FOV) positioned in the region of the cerebrum. To correct for photon attenuation, low-dose CT imaging was acquired in helical mode. The subject's head rested on a foam cushioned headrest. A head strap was applied to minimize head movement.

1000 MBq [15O]H2O, synthesized on-line ([15O]CO2 + 4H2 → 2[15O]H2O + CH4) was injected intravenously into an antecubital vein via an automatic water injection system (AM WR01, JFE Technos, Yokohama, Japan). The system delivered a 10 ml bolus over 10 seconds at 1 ml/sec with both pre- and post- flush of an inert saline solution. Immediately after starting the administration, emission data were acquired over 20 minutes in three-dimensional list mode with a 25.6 cm axial FOV and sorted into 40 time frames (40 × 30 seconds).

All emission scans were normalized for detector inhomogeneity and corrected for random coincidences, dead time, scattered radiation, and photon attenuation. For optimization of images, the 40 frames of the dynamic emission scans were reconstructed using 3D-OSEM (Ordered-Subset Expectation Maximization) with 2 iterations and 28 subsets to optimize visual quality images. The resultant image quality allowed manual identification of regions of interest (ROIs). For the reconstruction algorithms, the data were collected in a 128 × 128 × 47 matrix with a voxel size of 2.0 × 2.0 × 3.27mm.

Data Analysis

The CT and PET image data were transferred to a Xeleris 1.1 workstation (GE Healthcare) for PET data analysis. Manually defined ROIs on the attenuation corrected axial images and CT images (lateral and third ventricle, cortex of occipital lobe) were used to obtain the time-activity data of the scans of each subject. The tissue activity concentration in each ROI was expressed as the standardized uptake value (SUV, g/ml), corrected for the subject's body weight and administrated dose of radioactivity. Each tissue time activity concentration was determined by fitting the data using the following equation:

$$y(t) = y_0 + a*\exp(-b*t),$$

where y_0 is the baseline SUV. Subsequently, the ratio between SUVs of ventricle and cortex was defined as the influx ratio. The numerical data were subjected to the Mann-Whitney-Wilcoxon rank sum test for group analysis.

Results

The results are shown in Table 1 and summarized in Figure 1. Water influx into CSF space in AD patients expressed as influx ratio (0.755 ± 0.089) was significantly reduced compared to both young controls (1.357 ± 0.185, $p < 0.001$) and senior controls (0.901 ± 0.253, $p < 0.05$). Furthermore, the influx ratio of senior controls compared to that in young control was significantly reduced ($p < 0.01$) as well. The observed large range of influx ratio (0.599-1.442) in the senior controls suggested that the reduction in water influx into CSF represented one of the aging processes.

Discussion

Fluid-filled canals surrounding perforating arteries and veins in the parenchyma of the brain was recognized as far back as the early era of modern medicine and became known as the Virchow Robin space, so named after the first two scientists who described the structure in detail, namely, Rudolph Virchow and Charles Philippe Robin[15,16]. It was soon identified that fluid in the Virchow Robin space may play a role similar to systemic lymphatic[4-8, 17]. Studies based on modern technologies have disclosed the physiological significance of Virchow Robin space and interstitial fluid flow, ranging from the regulation of regional blood flow to β-amyloid clearance during sleep[18,19].

Interstitial fluid within the Virchow Robin space is regulated by aquaporin 4 (AQP-4)[2,3,10], which is an isoform of the aquaporin family, the protein channel that enables the movement of water across biological membranes. Among three of the isoforms, namely AQP-1, AQP-4, and AQP-9, identified in mammals in vivo, AQP-4 is expressed most abundantly in the brain and has a specific distribution within subpial and perivascular endfeet of astrocytes[20]. In contrast to capillaries of the systemic system where AQP-1 is a critical component, AQP-1 within CNS capillaries is actively suppressed, presumably for proper functionality of the blood brain barrier (BBB) and its tight junction[21]. As a result, AQP-1 in the brain is uniquely found in the choroid plexus epithelium. AQP-9 is only scarcely expressed in the CNS and considered to have no

significant role. Water influx into the CSF system from the blood stream has been shown to be regulated by AQP-4, not AQP-1. The interstitial flow of the brain, the system which is equivalent to systemic lymphatics, is now considered to be an AQP-4 dependent system.[14]

The basic function of lymphatic is drainage of cellular debris subjected to molecular scrutiny before returning to venous circulation. Although it is difficult to judge that the observed reduction in water influx into the CSF system in AD patients is the primary abnormality or merely a secondary epiphenomenon associated with β-amyloid deposits in the brain, the observed large range of influx ratios in senior controls strongly suggest that reduction in water influx into the CSF itself represents one of the aging processes. β-amyloid has been shown to be essential for synaptic formation[22]. Nonetheless, excess β-amyloid can result in aggregation of the protein and, in turn, senile plaque formation. Drainage of β-amyloid by interstitial flow through the Virchow Robin space into CSF is likely to be critical for maintaining proper homeostasis between β-amyloid production and clearance. In this matter, the ventricular system plays a role similar to lymph nodes of the systemic lymphatic system for neutralizing potential β-amyloid toxicity. Indeed, prealbumin (also known as transthyretin), the protein abundantly present in CSF, is a chaperon for β-amyloid, and prevents β-amyloid's natural tendency of accumulating into plaques[9]. The delicate balance between β-amyloid production and its clearance appears to be a critical factor for maintaining proper neural function. Disruption in its homeostasis may play a critical role in the pathogenesis of senile plaque and, hence, development of Alzheimer's disease.

Acknowledgement

The study in part was presented at the 66th AAN Annual Meeting of the American Academy of Neurology, April 2014, Philadelphia, USA and Alzheimer's Imaging Consortium, July 2014, Copenhagen, Denmark.

Figure Legends

Figure 1

Schematic presentation of the results with mean (circle) and standard deviation (bar). Water influx into CSF space is expressed as influx ratio (IR): the ratio between the standardized uptake value (SUV, g/m) of the ventricle to that of cortex. IR in Alzheimer's disease patients (AD) is significantly reduced compared to both young controls ($p < 0.001$) and senior controls ($p < 0.05$). Note that there is no overlap in data points between AD and young controls. Reduction of influx ratio in senior controls compared to that in young control is found to be significant ($p< 0.01$) as well. A large range of influx ratio in senior controls suggests that the observed reduction likely represents one of the aging processes.

Table 1

	Age	Influx Ratio
Young	21	1.10620
	22	1.16180
	21	1.45009
	21	1.14260
	24	1.48959
	22	1.62079
	21	1.35608
	24	1.41213
	22	1.24990
	30	1.57873
Senior	60	0.68299
	63	0.92728
	69	0.81396
	65	1.44195
	74	1.03050
	78	0.59892
	63	1.03987
	68	1.27526
	63	1.05720
	68	0.94050
AD	63	0.86105
	59	0.69261
	71	0.73065
	84	0.88935
	71	0.70088
	80	0.84389
	63	0.62796
	73	0.74510
	61	0.79321
	79	0.66232